¹H, ¹³C, and ¹⁵N resonance assignment and secondary structure of the pheromone binding protein from the

agricultural pest Ostrinia furnacalis (OfurPBP2)

Salik R. Dahal, Jacob L. Lewellen, Bharat P. Chaudhary, Smita Mohanty

Key words: Ostrinia furnacalis, NMR assignment, Pheromone binding proteins (PBPs)

Abstract

Ostrinia furnacalis, a lepidopteran moth, is an invasive pest found in Asia, Australia, Africa and parts of the United

States. The Ostrinia furnacalis pheromone-binding protein2 (OfurPBP2), present in the male moth antenna, plays a

role in the detection of female-secreted pheromone in a process that leads to mating. To understand the structural

mechanism of pheromone binding and release in this pest, we have initiated characterization of OfurPBP2 by solution

NMR. Here, we report the backbone resonance assignments and the secondary structural elements of OfurPBP2 at

pH 6.5 using uniformly ¹³C, ¹⁵N-labeled protein with various triple resonance NMR experiments. The assignments

are 97 % completed for backbone and 88 % completed for side-chain resonances. The secondary structure of

OfurPBP2, based on backbone chemical shifts, consists of eight α-helices, including a well-structured C-terminal

helix.

Biological context

The lepidopteran moth Ostrinia furnacalis is a destructive pest to over three hundred crops, including corn, beans,

tomatoes, ginger, pepper, okra, and millet, causing 30% of yield losses in corn (Mazumder, Dahal et al. 2018).

Controlling this invasive pest in an environmentally friendly and species-specific manner is of great importance. Thus,

understanding the structural basis of the function of proteins involved in the olfactory pathway, where a chemical

signal evokes a behavioral response in males guiding them to the female for mating, is critical. A detailed

1

characterization of the mechanism of function of these olfactory proteins is essential in the development of novel mimics for these sex attractants.

The first step in this signaling cascade is the recognition and delivery of pheromones by pheromone-binding proteins (PBPs) to the odorant receptor located in the sensory neuron of male antennae. These small acidic proteins are present in high concentration in the sensillum lymph of male moth antennae. PBPs capture hydrophobic pheromones at the air-lymph interface and ferry them across the aqueous lymph to the odorant receptor. Biochemical and structural studies of several lepidopteran PBPs, including *Bombyx mori* PBP (BmorPBP)(Damberger, Nikonova et al. 2000, Horst, Damberger et al. 2001, Lee, Damberger et al. 2002) *Antheraea polyphemus* pheromone-binding protein1 (ApolPBP1)(Mohanty, Zubkov et al. 2003, Mohanty, Zubkov et al. 2004, Zubkov, Gronenborn et al. 2005, Damberger, Ishida et al. 2007), *Amyelois transitella* PBP1 (AtraPBP1)(Xu, Xu et al. 2010, Xu, Xu et al. 2011, di Luccio, Ishida et al. 2013), and *Lymantria dispar* PBP2 (LdisPBP2)(Kowcun, Honson et al. 2001), show that these proteins bind their respective pheromone at the relatively high pH (> 6.0) of the sensillar lymph and release them at a lower pH (<5.0) present near the membrane-bound receptor. The pheromones occupy the hydrophobic binding pockets at higher pH for these proteins when their C-termini are exposed to the solvent as random coils. However, at lower pH, the C-termini switch to helices and occupy the binding pocket, releasing the ligands near the receptor.

We have reported for ApolPBP1 that the pH-dependent conformational switch is regulated by two biological gates: a histidine gate consisting of His70 and His95 at one end of the binding pocket and a C-terminal gate regulated by the C-terminus of the protein at the other end. At higher pH (> 6.0), the histidine gate is shut while the C-terminal gate allows the ligand to enter and bind to the pocket (Katre, Mazumder et al. 2009). We have shown that the unstructured C-terminus of ApolPBP1 is indeed critical for ligand-binding at higher pH (Katre, Mazumder et al. 2013). At lower pH, the histidine gate opens due to charge repulsion between the two positively charged histidine residues, while the C-terminal gate shuts when the unstructured C-terminus switches to a helix and occupies the pocket, pushing the ligand out through the opened histidine gate (Katre, Mazumder et al. 2009, Katre, Mazumder et al. 2013). Although OfurPBP2 has over 50 % sequence similarity with ApolPBP1, BmorPBP, AtraPBP1 and LdisPBP2, there are major differences in the two biological gates. In the histidine gate, His70 is replaced by an Arg, and the C-terminal gate has

four additional charged residues. To understand the effect of these critical substitutions on the structure and function of OfurPBP2, we have initiated a detailed structural characterization by solution NMR. Here, we report backbone assignments of OfurPBP2 at pH 6.5.

Methods and Experiments

Uniformly labeled ¹⁵N-, and ¹⁵N/¹³C- labeled recombinant OfurPBP2 proteins were expressed in E. coli and purified by ion exchange and size exclusion chromatography as described previously (Mazumder, Dahal et al. 2018). The purity and mass were confirmed by SDS-PAGE and MALDI-TOF¹. NMR samples contained 0.4 mM uniformly ¹⁵Nand ¹⁵N/¹³C-labeled OfurPBP2 (95% H₂O/5 % D₂O) in 50 mM phosphate buffer (pH 6.5) containing 1 mM EDTA and 0.1% NaN₃. All NMR data were collected at 35 °C on a Bruker Avance II 800 fitted with a triple resonance H/C/N TCI cryoprobe at the National High Magnetic Field Laboratory (NHMFL) at Tallahassee, FL. The 2D {\frac{15}{N}}-\frac{1}{15}} HSQC spectrum (Fig. 1) was collected with 256 complex points in ¹⁵N dimension and 2048 complex points in ¹H dimension. The following experiments were used for sequential assignment of ${}^{1}HN$, ${}^{1}H_{\alpha}$, ${}^{15}N$, ${}^{13}C_{\alpha}$, ${}^{13}C_{\beta}$, and ${}^{13}CO$ resonances: 2D {15N,1H}-HSQC, 2D {13C,1H}-HSQC, 3D HNCA, 3D HN(CO)CA, 3D HNCO, 3D HN(CA)CO, 3D HNCACB, 3D CACB(CO)NH, 3D CC(CO)NH, 3D H(CCCO)NH, 3D HCCH-TOCSY, 3D 15N-edited HSQC TOCSY, and 3D ¹⁵N/¹³C-edited NOESY (with mixing times of 85 and 120 ms). Data were processed with NMRPipe (Delaglio, Grzesiek et al. 1995) and analyzed with NMRFAM-SPARKY (Lee, Tonelli et al. 2015). The 2D HSQC spectra collected at 20 and 55 °C suggested that OfurPBP2 is very stable, undergoing no apparent conformational changes. The secondary structure, as shown in Fig. 2, was obtained by TALOS+ (Shen, Delaglio et al. 2009). Secondary chemical shifts, ΔC_{α} and ΔC_{β} and $(\Delta C_{\alpha}-\Delta C_{\beta})$ as shown in Fig. 3, were calculated by subtracting random coil values from the C_{α} and C_{β} shifts (Wishart, Bigam et al. 1995).

Assignments and data deposition

The 2D $\{^{15}N^{-1}H\}$ -HSQC spectrum of OfurPBP2 at pH 6.5 exhibits well-dispersed $^{1}H^{-15}N$ resonances (**Fig. 1**). The protein exists as a monomer. The assignment of backbone resonances (^{1}HN , ^{15}N , $^{13}C\alpha$, $^{13}C_{\beta}$, and ^{13}CO) was completed for all residues in the 2D $\{^{15}N^{-1}H\}$ -HSQC except S1, Q2, and K143. All six cysteine residues were in the oxidized

state as indicated by their $^{13}C_{\beta}$ chemical shifts. The ϕ and ψ backbone torsional angles and the secondary structural elements were obtained from TALOS+ (**Fig. 2**). Based on TALOS+ calculations (**Fig. 2**), eight helical regions were observed in the following peptide segments of the protein: 3-23, 27-34, 46-58, 71-79, 84-96, 108-116,119-125, 131-141. The secondary structure elements were also calculated with secondary chemical shift: ΔC_{α} - ΔC_{β} , ΔC_{α} and $-\Delta C_{\beta}$ (**Fig. 3**). Again, eight α -helices were observed (**Fig. 3**).

A quick inspection of the secondary structure elements of OfurPBP2 shows that the C-terminus involving the peptide segment 131-141 has α-helical structure at pH 6.5 (**Figs. 2 and 3**). This observation is quite surprising, and contrasts strongly with previous reports for several well-studied lepidopteran PBPs, including ApolPBP1 (Mohanty, Zubkov et al. 2004), BmorPBP (Lee, Damberger et al. 2002), and AtraPBP1 (di Luccio, Ishida et al. 2013). The C-terminus of each of these PBPs exist as a coil that is exposed to the solvent in the ligand-bound conformation of the protein at pH>6.0. However, the ligand is released at a lower pH (<5.0) near the site of the olfactory receptor neuron through a pH-dependent conformational switch, where the C-terminus switches to a helix and outcompetes the pheromone for the pocket. We have reported previously that the structure of OfurPBP2 is adversely affected at a lower pH (<5.0), unlike the structures of ApolPBP1, BmorPBP, AtraPBP1, and LdisPBP2 (Mazumder, Dahal et al. 2018). Taken together, all the above data indicate that OfurPBP2 may have a novel mechanism of pheromone uptake and release that is different than other lepidopteran moth PBPs.

Both the backbone and side-chain chemical shift assignments have been deposited in the BioMagResBank (www. bmrb.wisc.edu) under accession number 50074.

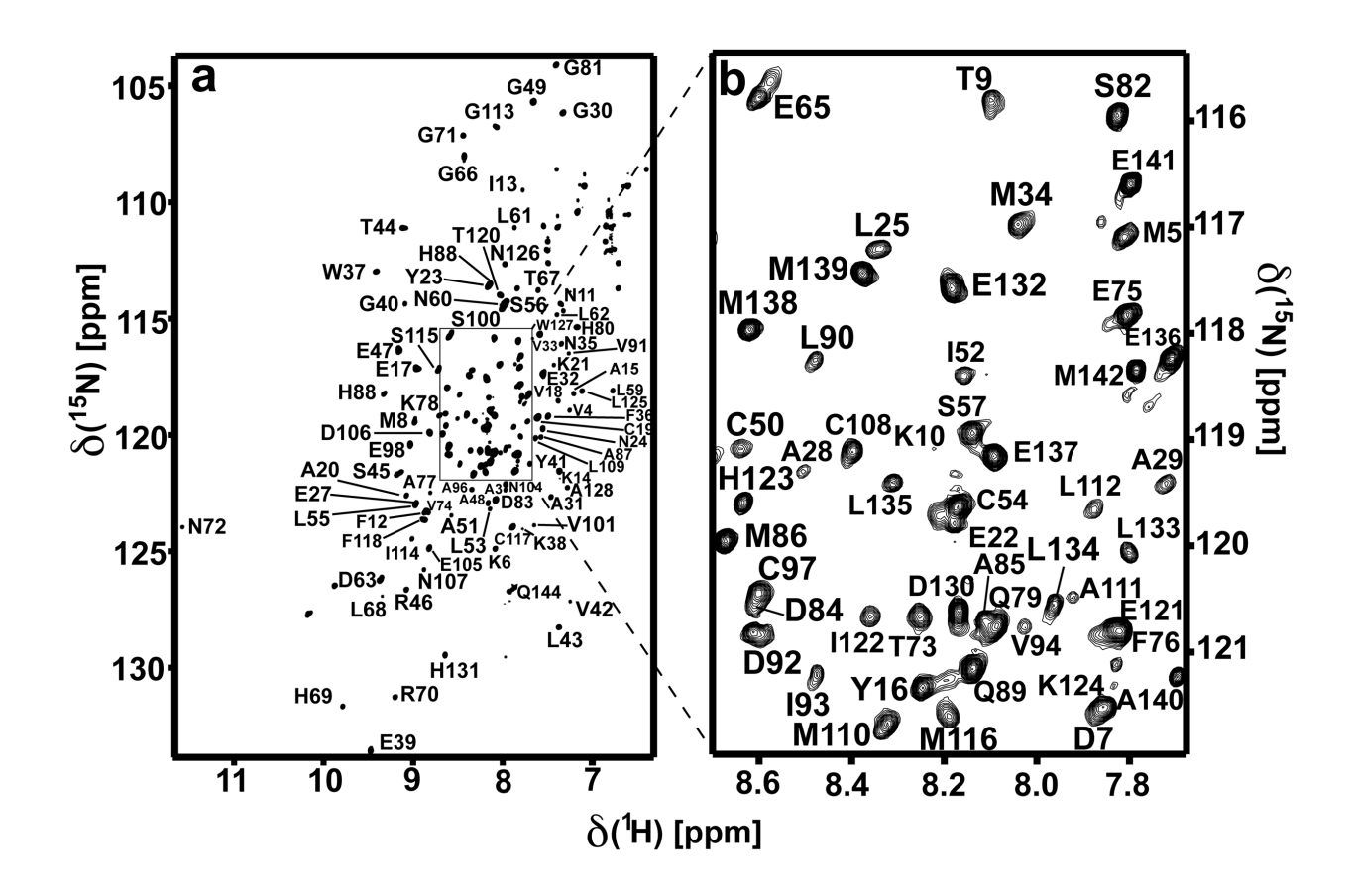


Fig 1: (a) 800 MHz 2D {\frac{15}{N}, \frac{1}{H}}-HSQC spectrum of uniformly \frac{15}{N}/\frac{13}{C}-enriched OfurPBP2 at pH 6.5 at 308 K. The primary structure of OfurPBP2 contains 144 residues. Backbone amide cross peaks have been labeled with residues type and sequence number. The residues S1, Q2, and K143 were not found in the spectra. Resonances of the side-chain glutamine and asparagine amide groups have not been labeled. (b) Expanded region of the HSQC spectrum shown in the rectangular inset.

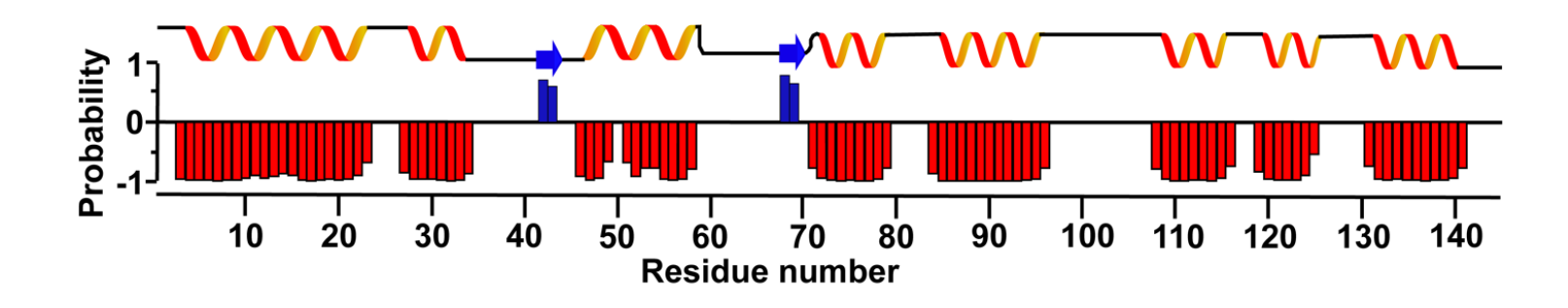


Fig 2: Secondary structure prediction of OfurPBP2 obtained with TALOS+¹⁴ using the ^{1}H , ^{15}N , $^{13}C_{\alpha}$, $^{13}C_{\beta}$, and $^{13}C'$ backbone chemical shifts. The secondary structure prediction is shown as red bars for α helices and blue bars for β strands, with the height of the bars representing the probability of the secondary structure (-1 for α-helix, 0 for random coil, 1 for β-strand).

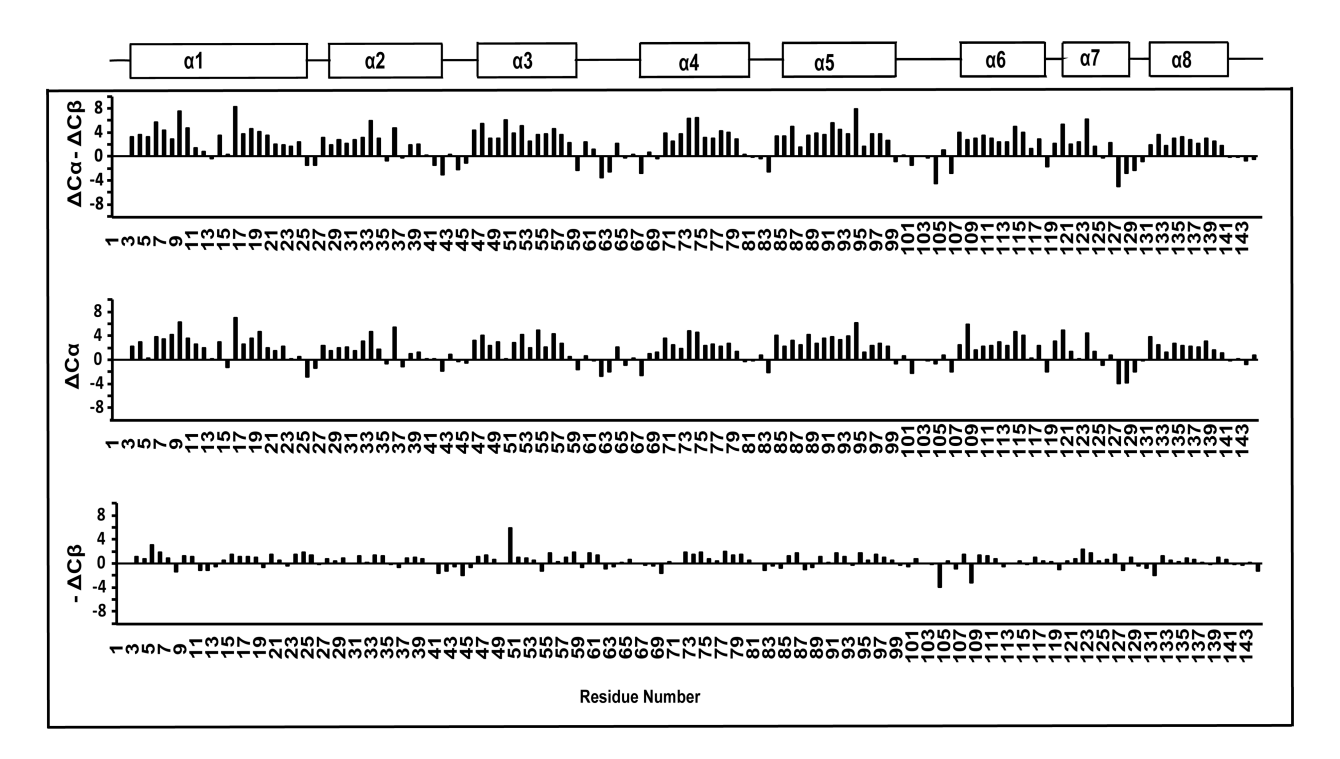


Fig 3: Secondary chemical shift, $\Delta C\alpha$ - $\Delta C\beta$, $\Delta C\alpha$ and - $\Delta C\beta$ are plotted against the linear amino acid sequence. $\Delta C\alpha$ and $\Delta C\beta$ are calculated by subtracting random coil values from the $C\alpha$ and $C\beta$ shift (Wishart, Bigam et al. 1995). The helical regions are shown at the top.

Acknowledgements

This research was financially supported by National Science Foundation Award CHE-1807722 to Smita Mohanty. We thank Dr. David Zoetewey for numerous useful discussions. All NMR data were collected at the National High Magnetic Field Laboratory, which is supported by National Science Foundation Cooperative Agreement No. DMR-1644779 and the State of Florida. We thank Dr. Thomas Webb of Auburn University for the critical reading of this manuscript.

Author Contributions

SM conceived, designed the strategies and techniques employed, supervised the research, and analyzed the data. SD and BC conducted NMR experiments. SD and JL processed and analyzed NMR data and completed the NMR resonance assignments. SM and SD wrote the paper and SD and JL prepared figures.

Compliance with ethical standards

Conflict of interest

The authors declare that they have no conflicts of interest with the contents of this article.

References

Damberger, F., et al. (2000). "NMR characterization of a pH-dependent equilibrium between two folded solution conformations of the pheromone-binding protein from Bombyx mori." Protein science: a publication of the Protein Society **9**(5): 1038-1041.

Damberger, F. F., et al. (2007). "Structural Basis of Ligand Binding and Release in Insect Pheromone-binding Proteins: NMR Structure of Antheraea polyphemus PBP1 at pH 4.5." Journal of Molecular Biology **373**(4): 811-819.

Delaglio, F., et al. (1995). "NMRPipe: a multidimensional spectral processing system based on UNIX pipes." Journal of biomolecular NMR **6**(3): 277-293.

di Luccio, E., et al. (2013). "Crystallographic observation of pH-induced conformational changes in the Amyelois transitella pheromone-binding protein AtraPBP1." PloS one **8**(2): e53840-e53840.

Horst, R., et al. (2001). "NMR structure reveals intramolecular regulation mechanism for pheromone binding and release." Proceedings of the National Academy of Sciences of the United States of America **98**(25): 14374-14379.

Horst, R., et al. (2001). "Letter to the Editor: NMR assignment of the A form of the pheromone-binding protein of Bombyx mori." Journal of biomolecular NMR **19**(1): 79-80.

Katre, U. V., et al. (2013). "Structural insights into the ligand binding and releasing mechanism of Antheraea polyphemus pheromone-binding protein 1: role of the C-terminal tail." Biochemistry **52**(6): 1037-1044.

Katre, U. V., et al. (2009). "Ligand binding turns moth pheromone-binding protein into a pH sensor: effect on the Antheraea polyphemus PBP1 conformation." J Biol Chem **284**(46): 32167-32177.

Kowcun, A., et al. (2001). "Olfaction in the gypsy moth, Lymantria dispar: effect of pH, ionic strength, and reductants on pheromone transport by pheromone-binding proteins." J Biol Chem **276**(48): 44770-44776.

Lee, D., et al. (2002). "NMR structure of the unliganded Bombyx mori pheromone-binding protein at physiological pH." FEBS Letters **531**(2): 314-318.

Lee, W., et al. (2015). "NMRFAM-SPARKY: enhanced software for biomolecular NMR spectroscopy." Bioinformatics (Oxford, England) **31**(8): 1325-1327.

Mazumder, S., et al. (2018). "Structure and Function Studies of Asian Corn Borer Ostrinia furnacalis Pheromone Binding Protein2." Sci Rep **8**(1): 17105.

Mohanty, S., et al. (2003). "1H, 13C and 15N backbone assignments of the pheromone binding protein from the silk moth Antheraea polyphemus (ApolPBP)." Journal of biomolecular NMR **27**(4): 393-394.

Mohanty, S., et al. (2004). "The Solution NMR Structure of Antheraea polyphemus PBP Provides New Insight into Pheromone Recognition by Pheromone-binding Proteins." Journal of Molecular Biology **337**(2): 443-451.

Mohanty, S., et al. (2004). "The solution NMR structure of Antheraea polyphemus PBP provides new insight into pheromone recognition by pheromone-binding proteins." J Mol Biol **337**(2): 443-451.

Shen, Y., et al. (2009). "TALOS+: a hybrid method for predicting protein backbone torsion angles from NMR chemical shifts." Journal of biomolecular NMR **44**(4): 213-223.

Wishart, D. S., et al. (1995). "1H, 13C and 15N random coil NMR chemical shifts of the common amino acids. I. Investigations of nearest-neighbor effects." Journal of Biomolecular NMR **5**(1): 67-81.

Xu, W., et al. (2011). "Extrusion of the C-terminal helix in navel orangeworm moth pheromone-binding protein (AtraPBP1) controls pheromone binding." Biochemical and Biophysical Research Communications **404**(1): 335-338.

Xu, X., et al. (2010). "NMR structure of navel orangeworm moth pheromone-binding protein (AtraPBP1): implications for pH-sensitive pheromone detection." Biochemistry **49**(7): 1469-1476.

Zubkov, S., et al. (2005). "Structural consequences of the pH-induced conformational switch in A.polyphemus pheromone-binding protein: mechanisms of ligand release." J Mol Biol **354**(5): 1081-1090.